




Spatially Coupled LDPC Codes via Partial Superposition and Their Application to HARQ

Qianfan Wang , *Student Member, IEEE*, Suihua Cai, Wenchao Lin, Shancheng Zhao, Li Chen , *Senior Member, IEEE*, and Xiao Ma , *Member, IEEE*

Abstract—This paper proposes a new class of spatially coupled codes, which are constructed by sending codewords of a low-density parity-check block code (LDPC-BC) in a block Markov superposition transmission (BMST) manner, resulting in the BMST-LDPC codes. Different from the conventional spatially coupled LDPC (SC-LDPC) codes, the proposed BMST-LDPC codes can have encoder/decoder implemented using the structure of the corresponding LDPC-BCs. The proposed construction is *universal*, which is applicable to any existing LDPC-BCs including the 5 G New Radio (5G-NR) LDPC-BCs to obtain extra coding gains. The proposed BMST-LDPC codes are also a special class of BMST codes, which have lower error floors even with an encoding memory of one, inheriting a low decoding latency. Moreover, *partial superposition*, where a fraction of the coded bits are superimposed onto the following codewords, is introduced to alleviate the decoding error propagation. The construction can be optimized, for random long codes, by a protograph-based extrinsic information transfer (EXIT) chart analysis, or by a one-dimensional search for structured block codes. Furthermore, the BMST-LDPC scheme is integrated with the hybrid automatic retransmission request (HARQ) over the block fading channel, improving the throughput performance. Numerical results are presented to validate our analysis and demonstrate the performance advantage of the BMST-LDPC codes over the LDPC-BCs. They also show that the proposed HARQ scheme can yield a throughput improvement of up to 10% over the conventional HARQ scheme.

Index Terms—5G-NR, block markov superposition transmission (BMST), HARQ, LDPC, partial superposition, SC-LDPC.

I. INTRODUCTION

LOW-DENSITY parity-check block codes (LDPC-BCs), which were first introduced by Gallager [1] and rediscovered by Mackay, Neal and Spielman [2], [3], have been shown to be capacity-approaching [4] over the additive white Gaussian noise (AWGN) channel. Due to their good performance and high decoding throughput, the rate-compatible raptor-like LDPC-BCs have been adopted as the coding scheme for data channels in 5 G enhanced mobile broadband (eMBB) scenario [5]. Evidently, for the LDPC-BC coded systems, the transmissions of codewords at different time slots are independent and the decoding latency relies on the codeword length. In some applications such as downloading large files, the latency constraint can be relaxed. One would hope to improve the performance of the existing LDPC-BCs by tolerating an increased decoding latency while maintaining the similar encoder/decoder structures. This can be achieved by employing a coded transmission strategy called block Markov superposition transmission (BMST) [6], [7].

The BMST scheme introduces memory by spatially coupling the generator matrices of the basic codes to improve the performance, where the performance can be predicted by a simple lower bound [6]. The construction of the BMST scheme is flexible since the construction can be tailored to adapt to any given (rational) code rate and any target error rate [7]. However, the original BMST codes do not perform well over the block fading channel due to error propagation. To overcome this weakness, systematic BMST of repetition (BMST-R) [8] codes were proposed, where only parity-check bits are superimposed onto the adjacent transitions in the BMST manner, following the idea of *partial superposition* in [9] for nested lattice codes. Similarly, partial superposition has also been employed in multiplicative repetition superposition transmission codes [10], [11] to alleviate error propagation. The above BMST strategies can improve the performance over the basic codes while the hardware structure of the data processors can still be designed with a core of the underlying basic codes.

Integrating the BMST scheme and partial superposition, we present a new class of BMST codes, called the BMST-LDPC codes, as an extension of [12]. The BMST-LDPC codes

Manuscript received July 18, 2020; revised January 10, 2021 and February 28, 2021; accepted March 2, 2021. Date of publication March 9, 2021; date of current version May 5, 2021. This work was supported in part by the National Key R&D Program of China under Grant 2020YFB1807100, in part by the National Natural Science Foundation of China under Grants 61971454 and 62071498, in part by the Science and Technology Planning Project of Guangdong Province under Grant 2018B010114001, and in part by the Shenzhen Municipal Commission of Science and Innovation. This paper was presented at the 2019 IEEE International Symposium on Information Theory. The review of this article was coordinated by Prof. H. Nguyen. (*Corresponding author: Xiao Ma.*)

Qianfan Wang is with the School of Electronics and Communication Engineering, Sun Yat-sen University, Guangzhou 510006, China (e-mail: wangqf6@mail2.sysu.edu.cn, wangqf6@mail2.sysu.edu.cn).

Suihua Cai, Wenchao Lin, and Xiao Ma are with the School of Computer Science and Engineering and Guangdong Key Laboratory of Information Security Technology, Sun Yat-sen University, Guangzhou 510006, China (e-mail: caish23@mail.sysu.edu.cn; linwch7@mail2.sysu.edu.cn; maxiao@mail.sysu.edu.cn,).

Shancheng Zhao is with the College of Information Science and Technology, Jinan University, Guangzhou 510632, China, and also with the Guangdong Key Laboratory of Data Security and Privacy Preserving, Jinan University, Guangzhou 510632, China (e-mail: shanchengzhao@jnu.edu.cn).

Li Chen is with the School of Electronics and Information Technology, Sun Yat-sen University, Guangzhou 510006, China (e-mail: chenli55@mail.sysu.edu.cn).

Digital Object Identifier 10.1109/TVT.2021.3065052

are similar to the spatially coupled LDPC (SC-LDPC) codes. The SC-LDPC codes, also known as LDPC convolutional codes, were first introduced in [13] and have asymptotically capacity-achieving performance over binary memoryless symmetric (BMS) channels under the iterative belief propagation (BP) decoding [14]. This is due to the so-called *threshold saturation*, where the BP decoding performance of SC-LDPC codes can approach the maximum *a posteriori* (MAP) decoding performance of the underlying LDPC-BCs [15], [16]. The SC-LDPC codes can be decoded by a sliding-window (SW) decoder [15], [17], which has a low decoding latency. As a result, the construction of the SC-LDPC codes has received significant attention in recent years, including the unwrapping procedure [13] and the protograph approach [18], [19]. Most constructions can be carefully tailored to avoid short cycles or trapping sets in the Tanner graph [20]–[23], resulting in an improved performance especially in the error floor region. For example, a systematic protograph-based construction was proposed in [24] such that the Tanner graph can have a girth of at least eight, the replicate-and-mask construction was proposed in [25] to improve the performance in the finite-length regime, and a multiple-edge protograph-based construction was proposed in [26] with a girth of eight.

In this paper, we propose the BMST-LDPC codes, which not only preserve the advantages of the original BMST codes, including low encoding complexity, effective SW decoding, low implementation complexity and predictable error floors, but also have better performance even with an encoding memory of one and hence inherit a lower decoding latency. The main contributions of this paper include:

- 1) We present a new class of BMST codes, which are constructed by sending codewords of an LDPC-BC in a BMST manner. On the premise of similar performance in the waterfall region, the construction of the BMST-LDPC codes is *universal* since it is applicable to any existing LDPC-BCs, e.g., the 5G New Radio (5G-NR) LDPC-BCs to obtain extra coding gains. In addition, the BMST-LDPC codes can be easily implemented with the hardware structure of the underlying LDPC-BCs.
- 2) To avoid catastrophic error propagation, we propose to use *partial superposition* characterized by a parameter called *superposition fraction*, in which only a portion of the coded bits are selected and superimposed onto the following codewords.
- 3) A protograph-based extrinsic information transfer (EXIT) chart analysis is presented to predict the optimal superposition fraction of the BMST-LDPC codes, so that the decoding performance can be maximized.
- 4) For practical wireless systems, we propose to integrate partial superposition transmission of LDPC codewords with the hybrid automatic retransmission request (HARQ) scheme, resulting in a throughput-enhanced HARQ scheme, called the BMST-LDPC HARQ scheme.
- 5) Our numerical results show that the BMST-LDPC codes can yield an extra coding gain of up to 1 dB over the underlying LDPC-BCs. The BMST-LDPC HARQ scheme can yield a throughput improvement of up to 10% over the conventional HARQ scheme.

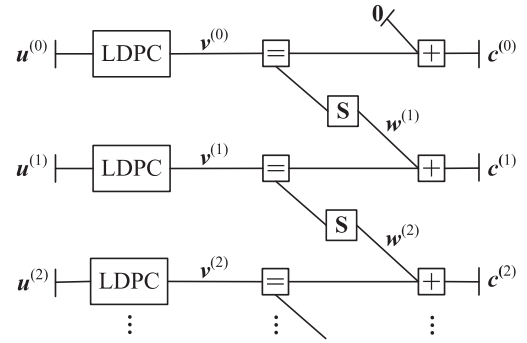


Fig. 1 Normal graph of a BMST-LDPC code.

Algorithm 1: Encoding of the BMST-LDPC Codes.

- *Initialization*: Set $v^{(-1)} = \mathbf{0} \in \mathbb{F}_2^n$.
 - *Recursion*: For $t = 0, 1, \dots, L - 1$,
 - 1) Encode $u^{(t)}$ into $v^{(t)}$ by the encoding algorithm of the basic LDPC-BC, i.e., $v^{(t)} = u^{(t)}\mathbf{G}$;
 - 2) Compute $w^{(t)} = v^{(t-1)}\mathbf{S}$, where \mathbf{S} is a selection matrix;
 - 3) Compute $c^{(t)} = v^{(t)} + w^{(t)}$, which is taken as the t -th block of transmission.
 - *Termination*: Set $c^{(L)} = v^{(L-1)}\mathbf{S}$, where only $n\alpha$ active bits of $c^{(L)}$ need to be transmitted.¹
-

II. BMST-LDPC CODES

A. Encoding Algorithms

Let $\mathcal{C}[n, k]$ denote a binary LDPC-BC of length n and dimension k , whose parity-check matrix and generator matrix are denoted by \mathbf{H} and \mathbf{G} , respectively. Advancing from original BMST codes, we take LDPC-BCs as basic codes and focus on the case of encoding memory one. The encoding memory is fixed to one due to the following reasons. First, our construction is based on well-constructed LDPC-BCs, which already have capacity-approaching performance. Further increasing memory will only lead to marginal performance improvement. Second, we attempt to keep the decoding complexity and latency as low as possible. Also note that, we consider BMST with partial superposition to alleviate error propagation.

Let α ($0 \leq \alpha \leq 1$) denote a *superposition fraction* that is to be optimized. We define a *selection matrix* \mathbf{S} by nulling $n(1 - \alpha)$ out of n columns of a given permutation matrix. For a binary vector $v \in \mathbb{F}_2^n$, $v\mathbf{S}$ is a vector that is an interleaving version of v but with some bits nulled. Given a sequence of data $\mathbf{u} = (u^{(0)}, u^{(1)}, \dots, u^{(L-1)})$ with $u^{(t)} = (u_0^{(t)}, u_1^{(t)}, \dots, u_{k-1}^{(t)}) \in \mathbb{F}_2^k$, the encoding algorithm has the same framework as for a general BMST code [6] and is described in Algorithm 1, see Fig. 1 for illustration. The main difference is the use of a selection matrix \mathbf{S} instead of a permutation matrix.

¹The code length is $n(L + \alpha)$ and the real code rate is then $k/n \cdot L/(L + \alpha) \approx k/n$ for $L \gg 1$. Nevertheless, we will treat the code length as $n(L + 1)$ for notational convenience in the rest of this paper.

B. Algebraic Description of BMST-LDPC Codes

In this subsection, the relations between the presented codes and the existing codes are revealed by their algebraic descriptions. With termination, a BMST of $\mathcal{C}[n, k]$ LDPC-BC with a superposition fraction α can be treated as a linear block code with dimension kL and length $n(L + 1)$. The generator matrix of the BMST-LDPC code can be specified as a banded block matrix,

$$\mathbf{G}_{\text{BMST-LDPC}} = \begin{bmatrix} \mathbf{G} & \mathbf{GS} & & & & \\ & \mathbf{G} & \mathbf{GS} & & & \\ & & \ddots & \ddots & & \\ & & & \mathbf{G} & \mathbf{GS} & \\ & & & & & \end{bmatrix},$$

where \mathbf{G} is the generator matrix of the basic LDPC-BC and \mathbf{S} is a selection matrix.

Similar to the derivation in [6], we can determine the parity-check matrix of the BMST-LDPC code as a lower block-triangular matrix,

$$\mathbf{H}_{\text{BMST-LDPC}} = \begin{bmatrix} \mathbf{H} & & & & & \\ \mathbf{HS}_1 & \mathbf{H} & & & & \\ \mathbf{HS}_2 & \mathbf{HS}_1 & \mathbf{H} & & & \\ \vdots & \vdots & \vdots & \ddots & & \\ \mathbf{HS}_{L-1} & \mathbf{HS}_{L-2} & \mathbf{HS}_{L-3} & \cdots & \mathbf{H} & \\ \mathbf{S}_L & \mathbf{S}_{L-1} & \mathbf{S}_{L-2} & \cdots & \mathbf{S}_1 & \mathbf{I} \end{bmatrix},$$

where \mathbf{H} is the parity-check matrix of the basic LDPC-BC and $\mathbf{S}_i = (\mathbf{S}^i)^T$ for $i \geq 1$. By construction, we know that the selection matrix \mathbf{S} has $n(1 - \alpha)$ zero columns and hence $n(1 - \alpha)$ zero rows. So, \mathbf{S}_i has at least $n(1 - \alpha)$ zero columns, and \mathbf{HS}_i is a low-density matrix.

As demonstrated in [27], BMST-LDPC codes can be viewed as a chain of L independent LDPC-BCs coupled by superposition. There are obvious similarities between BMST-LDPC codes and SC-LDPC codes. However, distinguished from SC-LDPC codes, BMST-LDPC codes have their own features.

- The BMST-LDPC codes are constructed by spatially coupling the generator matrices of LDPC-BCs, and hence the generator matrix of the BMST-LDPC codes is a banded block matrix. In contrast, the SC-LDPC codes are constructed by spatially coupling the parity-check matrices of LDPC-BCs, and hence the parity-check matrix of the SC-LDPC codes is a banded block matrix.
- For the BMST-LDPC codes, all-zero sequences can be employed to force the encoders into the zero state at the termination procedure. While for the SC-LDPC codes, the termination procedure is usually implemented with a non-zero sequences which depends on the encoded information bits [28]. Therefore, in comparison with the conventional SC-LDPC codes, the termination procedure of the BMST-LDPC codes is simpler.
- The conventional SC-LDPC codes are typically constructed based on protograph and hence have a number of widely discussed characteristics such as linear distance

growth rate and the threshold saturation effect. In contrast, the BMST-LDPC codes are constructed based on well-designed LDPC-BCs and hence the linear distance growth rate and the threshold saturation effect are out of the question. However, we found by simulation (not included in this paper due to the space limitation) that the BMST-LDPC codes do have decoding waves similar to the SC-LDPC codes. Intuitively, for the BMST-LDPC codes with termination, the first layer and the last layer should have better performance because the “interference” from other layers to these two layers is less.

As a special class of BMST codes, the BMST-LDPC codes have their own features.

- Partial superposition, as opposed to full superposition, is used in the BMST-LDPC codes. Taking any existing well-designed LDPC-BC as the basic code, we can easily obtain an extra coding gain by optimizing α .
- The BMST-LDPC codes have a lower error floor even with an encoding memory of one and hence have a lower decoding latency.
- The parity-check based stopping criterion, as opposed to the entropy-based stopping criterion, can be used in the BMST-LDPC codes, which has lower complexity and will be mentioned in the following decoding algorithm.

C. Decoding Algorithms

Assume that $\mathbf{c}^{(t)}$ is transmitted through a channel, resulting in a received vector $\mathbf{y}^{(t)}$ at the receiver. We can compute the *a posteriori* probabilities or log-likelihood ratios (LLRs) associated with $\mathbf{c}^{(t)}$ from $\mathbf{y}^{(t)}$ as the input of the SW decoding algorithm. In particular, by assuming that the channel state information (CSI) is known at the receiver for the fading channel, the LLRs associated with $\mathbf{c}^{(t)}$ can be calculated as

$$\text{LLR}(c_i^{(t)}) = \ln \frac{\Pr\{y_i^{(t)} | c_i^{(t)} = 0, h\}}{\Pr\{y_i^{(t)} | c_i^{(t)} = 1, h\}}, \quad (1)$$

for $0 \leq i \leq n - 1$, where h denotes the Rayleigh fading coefficient. As a special class of BMST codes, BMST-LDPC codes can be decoded by the iterative SW decoding algorithm over a normal graph [29]. Fig. 1 shows the *high-level* normal graph of a BMST-LDPC code. The iterative SW decoding algorithm can be described as a message-passing algorithm over a subgraph of Fig. 1 containing d (the window size) layers, leading to a decoding latency of dn bits. Each decoding layer consists of a node of type $\boxed{+}$, a node of type $\boxed{\mathbf{S}}$, a node of type $\boxed{=}$, and a node of type $\boxed{\text{LDPC}}$. The message-updating rules of these nodes are outlined below.

- Node $\boxed{+}$: This node represents the constraint that the sum of all connecting variables must be zero over \mathbb{F}_2 . The message-updating rule at this node is similar to that at the check node in an LDPC-BC. The only difference is that the messages associated with the half edges are calculated from the channel observations.
- Node $\boxed{\mathbf{S}}$: This node represents the selection matrix, which simply transfers the messages associated with the selected bits between the node $\boxed{=}$ and the node $\boxed{+}$.

Algorithm 2: Iterative Sliding-Window Decoding of the BMST-LDPC Codes (Window Size $d \geq 1$).

- *Global initialization:* Set a maximum global iteration number $J_{\max} > 0$. For $0 \leq t \leq d - 2$, compute the LLRs associated with $c^{(t)}$ from the received vector $\mathbf{y}^{(t)}$. All messages over the other edges within and connecting to the t -th layer ($0 \leq t \leq d - 2$) are initialized as uniformly distributed variables.
- *Sliding-window decoding:* For $t = 0, 1, \dots, L - 1$,
 - 1) *Local Initialization:* If $t + d - 1 \leq L$, compute the LLRs from the received vector $\mathbf{y}^{(t+d-1)}$ and all messages over other edges within and connecting to the $(t + d - 1)$ -th layer are initialized as uniformly distributed variables.
 - 2) *Iteration:* For $j = 1, 2, \dots, J_{\max}$,
 - a) *Forward recursion:* For $i = 0, 1, \dots, d - 1$, the $(t + i)$ -th layer performs a message-passing algorithm scheduled as

$$\boxed{+} \rightarrow \boxed{=} \rightarrow \boxed{\text{LDPC}} \rightarrow \boxed{=} \rightarrow \boxed{\text{S}}.$$
 - b) *Backward recursion:* For $i = d - 1, d - 2, \dots, 0$, the $(t + i)$ -th layer performs a message-passing algorithm scheduled as

$$\boxed{=} \rightarrow \boxed{\text{LDPC}} \rightarrow \boxed{=} \rightarrow \boxed{+} \rightarrow \boxed{\text{S}}.$$
 - c) *Decisions:* Make decisions on $\mathbf{v}^{(t)}$ resulting in $\hat{\mathbf{v}}^{(t)}$. If $\mathbf{H}\hat{\mathbf{v}}^{(t)} = \mathbf{0}$, exit the iteration. Notice that the parity-check stopping criterion is also used in the above recursions, where the node $\boxed{\text{LDPC}}$ performs an iterative BP decoding with a preset maximum iteration number I_{\max} .
 - 3) *Successive Cancellation:* Output $\hat{\mathbf{u}}^{(t)}$ based on $\hat{\mathbf{v}}^{(t)}$ and remove the effect of $\hat{\mathbf{v}}^{(t)}$ on $\mathbf{y}^{(t+1)}$.

- Node $\boxed{=}$: This node represents the constraint that all connecting variables must take the same value. The message-updating rule at this node is the same as that at the variable node in an LDPC-BC.
- Node $\boxed{\text{LDPC}}$: This node represents the LDPC-BC encoding constraint, where $\mathbf{v}^{(t)}$ must be a codeword corresponding to $\mathbf{u}^{(t)}$. The message updating at this node can be implemented based on certain soft-input soft-output (SISO) decoder, say, the sum-product algorithm (SPA) with a maximum iteration number I_{\max} , of the LDPC-BC. The extrinsic messages associated with $\mathbf{u}^{(t)}$ can be used to make decisions on the transmitted data.

The SW decoding algorithm is outlined in Algorithm 2 for completeness, which is the same as Algorithm 3 in [6], with the exception that the message updating at the basic code is implemented as an iterative (usually sub-optimal) SISO decoder of the LDPC-BC. Also note that the parity-check based criterion, as opposed to the entropy-based criterion, can be used to stop the iteration earlier.

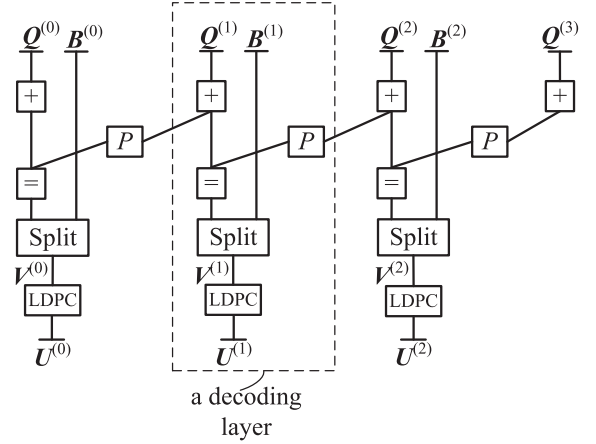


Fig. 2. Degenerated normal graph of a BMST-LDPC code.

D. Superposition Fraction Optimization

From the construction, we see that the superposition of $\mathbf{v}^{(t)}$ on $\mathbf{v}^{(t+1)}$ is helpful for the t -th layer but harmful for the $(t + 1)$ -th layer. Intuitively, this can be understood by noticing that the superposition brings “diversity” for the t -th layer but “interference” for the $(t + 1)$ -th layer. Hence, it is expected to obtain extra coding gain by optimizing α .

Such an optimization is a one-dimensional search problem, which can be solved by simulations. For random long codes, the time-consuming simulations can be avoided by invoking the EXIT chart analysis. The protograph-based EXIT chart analysis was proposed in [30] to obtain the threshold of the protograph-based LDPC codes.² The threshold is the minimum value of the signal-to-noise ratio (SNR) such that the error rate tends to zero at the variable nodes as the number of iterations increases. A modified EXIT chart analysis was proposed in [27] for the BMST codes when the repetition code or the single parity-check (SPC) code is chosen as the basic code. This situation becomes different when the basic code is an LDPC-BC and partial superposition is introduced. Based on the modified EXIT chart analysis, we present the EXIT chart analysis for the BMST-LDPC codes to predict the optimal superposition fraction. To simplify the analysis, the selection matrix is confined to have the following form

$$\mathbf{S} = \begin{bmatrix} \mathbf{P} & \mathbf{O} \\ \mathbf{O} & \mathbf{O} \end{bmatrix}, \quad (2)$$

where the sub-matrix \mathbf{P} of size $n\alpha \times n\alpha$ is uniformly picked from the set of all possible permutation matrices and \mathbf{O} represents the zero matrix. Taking the above form of \mathbf{S} into consideration, the degenerated normal graph of the BMST-LDPC codes is shown in Fig. 2, where $\mathbf{Q}^{(t)}$ is referred to as the superimposed part and $\mathbf{B}^{(t)}$ is referred to as the direct transmission part, yielding a ratio of $\frac{\alpha}{1-\alpha}$.

We assume that binary phase-shift keying (BPSK) modulation is used over the binary-input AWGN channel. For a given SNR

²The protograph-based EXIT chart analysis is also applicable to SC-LDPC codes to optimize the asymptotic performance, for example, see [31].

E_b/N_0 , where E_b denotes the transmitted energy per information bit and N_0 denotes the noise power spectral density, the channel bit LLRs also exhibit Gaussian distribution with variance [32],

$$\sigma_{\text{ch}}^2 = 8R_{\text{BMST-LDPC}} \frac{E_b}{N_0}. \quad (3)$$

The channel mutual information (MI) is then defined as

$$I_{\text{ch}} = J(\sigma_{\text{ch}}) = J\left(\sqrt{8R_{\text{BMST-LDPC}} \frac{E_b}{N_0}}\right), \quad (4)$$

where the $J(\cdot)$ function is given in the Appendix of [33].

The EXIT chart analysis of BMST-LDPC codes is performed over the normal graph, as shown in Fig. 2. We use the notation $I^{(a \rightarrow b)}$ to denote the MI from node \boxed{a} to node \boxed{b} . The MI message-passing algorithms of the nodes $\boxed{+}$, $\boxed{=}$ and \boxed{P} are the same as those in [27]. For the node $\boxed{\text{LDPC}}$, we employ the EXIT analysis algorithm corresponding to the underlying LDPC-BCs. The MI message-passing algorithms of the node $\boxed{\text{Split}}$, which is determined by the superposition fraction α , consists of the combination and partition. For the combination, the node $\boxed{\text{Split}}$ takes $I^{(=\rightarrow\text{Split})}$ and $I^{(\rightarrow\text{Split})}$ as input and delivers $I^{(\text{Split}\rightarrow\text{LDPC})}$ as the output, where $I^{(=\rightarrow\text{Split})}$, $I^{(\rightarrow\text{Split})}$ and $I^{(\text{Split}\rightarrow\text{LDPC})}$ denote the MI of the superimposed part, the direct transmission part and the output, respectively. The $I^{(\text{Split}\rightarrow\text{LDPC})}$ is then given by

$$I^{(\text{Split}\rightarrow\text{LDPC})} = \alpha I^{(=\rightarrow\text{Split})} + (1 - \alpha) I^{(\rightarrow\text{Split})}. \quad (5)$$

For the partition, the node $\boxed{\text{Split}}$ takes $I^{(\text{LDPC}\rightarrow\text{Split})}$ as the input and delivers $I^{(\text{Split}\rightarrow=)}$ and $I^{(\text{Split}\rightarrow\rightarrow)}$ as the output, where $I^{(\text{LDPC}\rightarrow\text{Split})}$, $I^{(\text{Split}\rightarrow=)}$ and $I^{(\text{Split}\rightarrow\rightarrow)}$ denote the MI of the input, the output to the superimposed part and the output to the direct transmission part, respectively. The output MI $I^{(\text{Split}\rightarrow=)}$ and $I^{(\text{Split}\rightarrow\rightarrow)}$ are given by

$$I^{(\text{Split}\rightarrow=)} = \alpha I^{(\text{LDPC}\rightarrow\text{Split})}, \quad (6)$$

$$I^{(\text{Split}\rightarrow\rightarrow)} = (1 - \alpha) I^{(\text{LDPC}\rightarrow\text{Split})}. \quad (7)$$

The EXIT chart analysis algorithm of the BMST-LDPC codes is described in Algorithm 3, see Fig. 2 for reference. Note that the convergence check at node $\boxed{\text{LDPC}}$ is performed using Algorithm 2 in [27].

Fig. 3(a) shows our EXIT chart analysis for the BMST-LDPC codes with the (3, 6)-regular LDPC-BC as the basic code, where we observe that the superposition fraction $\alpha = 0.4$ is optimal in terms of the threshold analysis. This is further validated by simulation results of Fig. 3(b),³ where a rate-1/2 (3, 6)-regular LDPC-BC with a length of 1024 bits constructed by the progressive-edge-growth (PEG) algorithm [34] is used as the basic code. Compared with the independent transmission⁴ ($\alpha = 0$), the BMST-LDPC code with $\alpha = 0.4$ has about 1.0 dB gain

³Notice that as α grows to 1, the real code rate decreases but the performance gets worse. This is because excessive superposition increases error propagation for the sub-optimal decoding algorithm.

⁴Notice that the calculated threshold is consistent with that presented in [35].

Algorithm 3: EXIT Chart Analysis of BMST-LDPC Codes with Sliding-Window Decoding.

- Initialization: Set a maximum number of iterations $\mathcal{O}_{\text{max}} > 0$. All messages over those half-edges (connected to the channel) at nodes $\boxed{+}$ and $\boxed{\text{Split}}$ are initialized according to (4) with a given SNR E_b/N_0 , all messages over those half-edges at nodes $\boxed{\text{LDPC}}$ are initialized as 0, and all messages over the remaining full-edges are initialized as 0.
 - Sliding-Window Decoding: For $i = 1, 2, \dots, \mathcal{O}_{\text{max}} > 0$, in each window position, the d decoding layers perform a message-passing algorithm layer-by-layer scheduled as

$$\boxed{+} \rightarrow \boxed{=} \rightarrow \boxed{\text{Split}} \rightarrow \boxed{\text{LDPC}} \rightarrow \boxed{\text{Split}} \rightarrow \boxed{=} \rightarrow \boxed{P}.$$
 - Convergence Check: Perform a convergence check at node $\boxed{\text{LDPC}}$. If a failed local decoding is detected, the window decoding terminates. Otherwise, a successful local decoding is declared, the window is slid, and the decoding continues. A complete successful decoding for a given SNR E_b/N_0 and target BER is declared if and only if all layers have declared a successful decoding.
-

at the bit error rate (BER) of 10^{-5} . We need to point out that the proposed EXIT chart analysis for the BMST-LDPC codes is based on the assumptions of infinite code length and randomly chosen selection matrix \mathbf{S} . However, the simulation results validate that the optimized superposition fraction by the EXIT chart analysis is effective when the code length is finite and \mathbf{S} is randomly chosen but fixed. Asymptotically (in the high SNR region), the BMST-LDPC codes can approach a maximum extra coding gain as predicted by the so-called genie-aided (GA) bound [6], [12]. The GA bound can be obtained by assuming that all interferences from adjacent layers are known at the decoder, or equivalently, by simulating the considered BMST-LDPC code with $L = 1$.

III. BMST-LDPC HARQ SCHEME

In practice, many wireless channels are time-varying and the transmitter usually does not know the CSI. In this case, it is difficult to achieve sufficiently reliable transmission by just error-correction codes. The HARQ scheme, which is a combination of the error-correction codes at the physical layer and the ARQ protocol at the link layer, is a commonly used technique to ensure the reliability of data transmission in wireless communication. Throughput is one of the most important performance metrics to evaluate a HARQ scheme. There are mainly two ways to improve the throughput performance. One is based on single-packet design, including fixed-rate codes with repetition redundancy (RR) [36] and Chase combining [37] or rate-compatible (RC) codes [38] with incremental redundancy (IR) [39]. The other is based on multiple-packet design, e.g., the cross-packet coding HARQ schemes [40]–[43], the

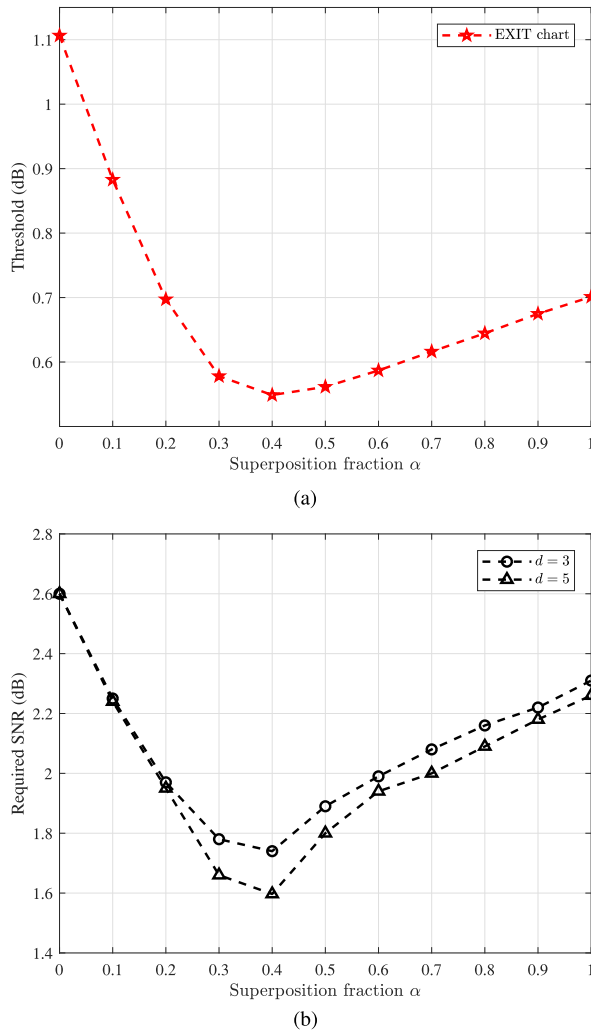


Fig. 3. The EXIT chart analysis and the required SNR E_b/N_0 in simulation corresponding to the target BER of 10^{-5} for the BMST-LDPC codes with different α . (a) EXIT chart analysis. (b) Simulation.

superposition-coding-aided HARQ schemes [44], [45], and the network-coded HARQ (NC-HARQ) schemes [46], [47].

In this section, we will show that partial superposition transmission of the LDPC codewords can also be combined with the RR-HARQ scheme to improve the throughput performance over the block fading channel. It is assumed that the Rayleigh fading coefficient h is constant over one block but has independent realizations at different blocks. For the sake of simplicity, we assume that the CSI is not known at the transmitter but perfectly known at the receiver. We also assume that the feedback channel is delay-free and error-free.

A. BMST-LDPC HARQ Scheme

We explain the basic idea of the BMST-LDPC HARQ scheme with the help of Fig. 4, where Alice attempts to send Bob a sequence of coded packets $\mathbf{v}^{(0)}, \mathbf{v}^{(1)}, \dots$, where $\mathbf{v}^{(t)} \in \mathbb{F}_2^n$. We only need to show how to successfully transmit $\mathbf{v}^{(0)}$. We assume that the first transmission of $\mathbf{v}^{(0)}$ is unsuccessful and a NACK is fed back from Bob to Alice.

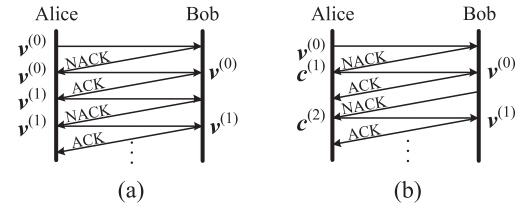


Fig. 4. Examples of conventional RR-HARQ scheme and BMST-LDPC HARQ scheme. (a) Conventional RR-HARQ. (b) BMST-LDPC HARQ.

For the conventional RR-HARQ scheme, as shown in Fig. 4(a), Alice retransmits $\mathbf{v}^{(0)}$ until an ACK is received or the maximum number of transmissions T_{\max} is reached. In contrast, for the BMST-LDPC HARQ scheme, as shown in Fig. 4(b), the first retransmission of $\mathbf{v}^{(0)}$ is given by

$$\mathbf{c}^{(1)} = \mathbf{v}^{(1)} + \mathbf{v}^{(0)}\mathbf{S}. \quad (8)$$

At the receiver, since both $\mathbf{v}^{(0)}$ and $\mathbf{c}^{(1)}$ carry information related to $\mathbf{v}^{(0)}$, their noisy versions can be employed to jointly recover $\mathbf{v}^{(0)}$ by performing the decoding algorithm (Algorithm 2 with $d = 2$) of the BMST-LDPC codes. If the decoding is successful, Bob feeds back an ACK. Otherwise, he feeds back a NACK. Upon receiving the second NACK, Alice retransmits $\mathbf{v}^{(0)}$ until an ACK is received or T_{\max} is reached. Meanwhile, the receiver turns into the single-packet mode and performs the SPA decoder of the LDPC-BC, where the input to the decoder is the up-to-date LLR vector that corresponds to $\mathbf{v}^{(0)}$ obtained by Chase combining. This is the main difference from the conventional RR-HARQ scheme. That is, retransmitting $\mathbf{v}^{(0)}$ brings no information of $\mathbf{v}^{(1)}$ to Bob in the conventional HARQ but an *extra* transmission of $\mathbf{v}^{(1)}$ in BMST-LDPC HARQ. Thus, it is expected for the BMST-LDPC HARQ scheme to have a higher throughput. We need to point out that the transmission of $\mathbf{c}^{(1)}$ will not be counted as a transmission of $\mathbf{v}^{(0)}$ but as that of $\mathbf{v}^{(1)}$. This is because, once $\mathbf{v}^{(0)}$ is recovered or T_{\max} is reached, the effect of $\mathbf{v}^{(0)}$ on $\mathbf{c}^{(1)}$ is removed and the received version of $\mathbf{c}^{(1)}$ will be reduced to a “noisy” version of $\mathbf{v}^{(1)}$.

We use $\ell_i^{(t)}$ to stand for LLR corresponding to the i -th coded bit and $\ell^{(t)}$ for the LLR vector. Let $\mathbf{v}^{(0)}, \mathbf{v}^{(1)}, \dots, \mathbf{v}^{(L-1)} \in \mathcal{C}[n, k]$ be L coded packets to be transmitted. The BMST-LDPC HARQ scheme is described in Algorithm 4.

Remarks: The lossless BMST-LDPC HARQ scheme means that the T_{\max} in Algorithm 4 is infinite and the truncated BMST-LDPC HARQ scheme means that the T_{\max} in Algorithm 4 is finite. In the truncated BMST-LDPC HARQ scheme, to mitigate the increasing complexity, the decoder does not try to decode $\mathbf{v}^{(t)}$ in the case when $\mathbf{v}^{(t)}$ is decoded incorrectly but $\mathbf{v}^{(t+1)}$ is decoded correctly.

B. Throughput Analysis of the BMST-LDPC HARQ Scheme

The long-term average throughput (LTAT) of a HARQ system is defined as the average number of correctly decoded information bits per transmitted symbol. Since the HARQ can be modelled as a Markov process, in which transmission rounds correspond to states and a HARQ cycle corresponds to a renewal

Algorithm 4: The BMST-LDPC HARQ Scheme.

Initialization: The transmitter transmits $\mathbf{v}^{(0)}$ and the receiver computes LLRs $\ell^{(0)}$;

for $t = 0, 1, \dots, L - 1$ **do**

The receiver decodes $\hat{\mathbf{v}}^{(t)}$ from $\ell^{(t)}$;

if $\hat{\mathbf{v}}^{(t)}$ is a valid codeword in \mathcal{C} **then**

The receiver feeds back an ACK;

The transmitter transmits $\mathbf{v}^{(t+1)}$ and the receiver computes LLRs $\ell^{(t+1)}$;

else

The receiver feeds back a NACK;

The transmitter transmits $\mathbf{c}^{(t+1)} = \mathbf{v}^{(t+1)} + \mathbf{v}^{(t)}\mathbf{S}$ and the receiver computes LLRs $\ell^{(t+1)}$;

The receiver performs the SW decoding algorithm (Algorithm 2), resulting in $\hat{\mathbf{v}}^{(t)}$;

while $\hat{\mathbf{v}}^{(t)}$ is not a valid codeword in \mathcal{C} and the number of transmissions $\mathbf{v}^{(t)}$ is less than T_{\max} **do**

The receiver feeds back a NACK;

The transmitter retransmits $\mathbf{v}^{(t)}$ and the receiver computes LLRs \mathbf{r} ;

The receiver updates $\ell^{(t)}$ by Chase combining, i.e., $\ell^{(t)} \leftarrow \ell^{(t)} + \mathbf{r}$, and performs the SPA of the LDPC-BC, resulting in $\hat{\mathbf{v}}^{(t)}$;

The receiver feeds back an ACK or a NACK depending on the decoding results and updates $\ell^{(t+1)}$ by removing the effect of $\mathbf{v}^{(t)}$;

cycle [42], the LTAT can be calculated using the renewal-reward theorem [48]. It is a ratio between the mean reward and the mean renewal time, where the mean reward is defined by the number of correctly decoded information bits per HARQ cycle and the mean renewal time is defined by the expected number of transmitted symbols per HARQ cycle. Let f_i denote the decoding failure probability in the i -th round after receiving the i -th transmission of $\mathbf{v}^{(0)}$. The probability of successful decoding in the i -th round is given by $f_{i-1} - f_i$. For the conventional lossless HARQ scheme, the throughput can be calculated as

$$\begin{aligned} \rho_c^{\text{lossless}} &= \frac{R(1 - f_1) + R(f_1 - f_2) + \dots}{1(1 - f_1) + 2(f_1 - f_2) + \dots} \\ &= \frac{R}{1 + \sum_{i=1}^{\infty} f_i}. \end{aligned} \quad (9)$$

In practice, for the conventional truncated HARQ scheme, where T_{\max} is finite, the throughput can be calculated as

$$\rho_c^{\text{truncated}} = \frac{R(1 - f_{T_{\max}})}{1 + \sum_{i=1}^{T_{\max}-1} f_i}. \quad (10)$$

For the lossless BMST-LDPC HARQ, we use f'_1 to denote the decoding failure probability after receiving $\mathbf{v}^{(0)}$ and $\mathbf{c}^{(1)}$. The decoding failure probabilities in other rounds are the same as those in the conventional lossless HARQ scheme. For the lossless BMST-LDPC HARQ scheme, the throughput can be calculated as

$$\rho_{\text{BMST}}^{\text{lossless}} = \frac{R(1 - f_1) + R(f_1 - f'_1) + R(f'_1 - f_2) + \dots}{1(1 - f_1) + 1(f_1 - f'_1) + 2(f'_1 - f_2) + \dots}$$

$$= \frac{R}{1 + f'_1 + \sum_{i=2}^{\infty} f_i}. \quad (11)$$

For the truncated BMST-LDPC HARQ scheme, where T_{\max} is finite, the LTAT can be estimated by

$$\rho_{\text{BMST}}^{\text{truncated}} \approx \frac{R(1 - f_{T_{\max}})}{1 + f'_1 + \sum_{i=2}^{T_{\max}-1} f_i}. \quad (12)$$

Therefore, based on (9)–(12), the throughput improvement of the BMST-LDPC HARQ can be obtained by choosing an appropriate superposition fraction α so that $f'_1 < f_1$.

IV. NUMERICAL RESULTS

In this section, we present our numerical results of the BMST-LDPC codes and the BMST-LDPC HARQ schemes. We use the (3, 6)-regular LDPC-BCs constructed by the PEG algorithm [34] and the 5G-NR LDPC-BCs as the basic codes. The SW decoding algorithm (Algorithm 2) is employed for the decoding. Unless otherwise stated, the maximum global iteration number is $J_{\max} = 50$ and the embedded basic LDPC-BCs are decoded by the SPA with a maximum iteration number of $I_{\max} = 1$. For independent LDPC-BCs, the maximum SPA iteration number is 50. The above setting ensures a similar decoding complexity between the BMST-LDPC codes and the independent LDPC-BCs. In all examples, earlier stopping is activated with the parity-check based stopping criterion. The encoder terminates every $L = 50$ sub-blocks in all simulations.

A. Comparison With the SC-LDPC Code

The following example is provided to compare the performance of a BMST-LDPC code and a (3, 6)-regular SC-LDPC code under the equal decoding latency constraint.

Example 1. (Comparison with the (3, 6)-regular SC-LDPC Code): Consider a rate-1/2 (3, 6)-regular LDPC-BC with a length of 1500 bits as the basic code. Codewords $\mathbf{c}^{(t)}$ are transmitted with BPSK modulation over the AWGN channel. The decoding window size of the BMST-LDPC codes is $d = 4$ and the decoding latency is 6000 bits. For comparison, we choose the (3, 6)-regular SC-LDPC code [49] with the same decoding latency. The maximum iteration numbers of the (3, 6)-regular SC-LDPC code are 10 and 20. Similarly, for the BMST-LDPC codes, $J_{\max} = 10$ or 20. The BER performance comparison is shown in Fig. 5, where we observe that the BMST-LDPC codes can perform as well as (or even better than) the (3, 6)-regular SC-LDPC code in the waterfall region. We need to point out that due to the forward recursion and backward recursion of the proposed decoding algorithm, the complexity per iteration of the BMST-LDPC codes is roughly twice as large as that of the conventional SC-LDPC codes. However, with the earlier stopping criterion specified by the underlying LDPC-BC, the BMST-LDPC codes may require less iteration numbers. Actually, we observe that the BMST-LDPC codes with $J_{\max} = 10$ can perform close to the (3, 6)-regular SC-LDPC codes with a maximum iteration number of 20 in the high SNR region.

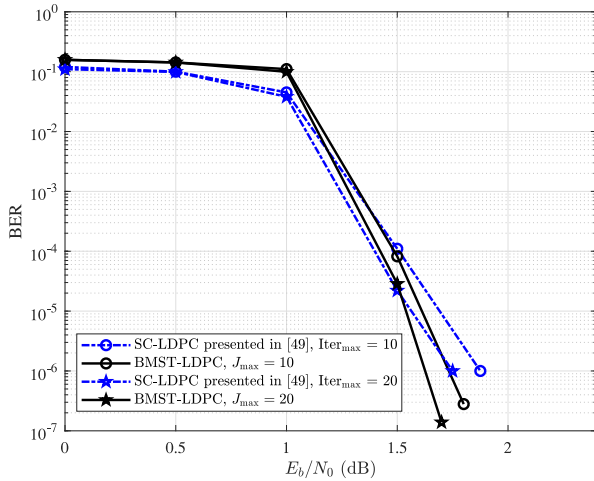


Fig. 5. BER performance of a BMST-LDPC code with real code rate about 0.496 and a (3, 6)-regular SC-LDPC code [49] with real code rate 0.490 in the same decoding latency of 6000 bits. For the BMST-LDPC code, the superposition fraction for encoding is $\alpha = 600/1500$, and the decoding window sizes are $d = 4$.

B. Improving the Performance of 5G-NR LDPC-BCs

For practical use, we employ the 5G-NR LDPC-BC as the basic code for the BMST-LDPC code to improve its performance. We consider the selection matrix \mathbf{S} with one of the following forms

$$\mathbf{S}_a = \begin{bmatrix} \mathbf{P} & \mathbf{O} \\ \mathbf{O} & \mathbf{O} \end{bmatrix}, \mathbf{S}_b = \begin{bmatrix} \mathbf{O} & \mathbf{P} \\ \mathbf{O} & \mathbf{O} \end{bmatrix},$$

$$\mathbf{S}_c = \begin{bmatrix} \mathbf{O} & \mathbf{O} \\ \mathbf{P} & \mathbf{O} \end{bmatrix}, \mathbf{S}_d = \begin{bmatrix} \mathbf{O} & \mathbf{O} \\ \mathbf{O} & \mathbf{P} \end{bmatrix}.$$

Example 2. (Varying Selection Matrices \mathbf{S}): The basic code is a rate-1/2 5G-NR LDPC-BC with a length of 1920 bits, which is constructed based on BG2 [50] with the lifting factor $Z = 96$. Codewords $c^{(t)}$ are transmitted with BPSK modulation over the AWGN channel. The window size is $d = 3$. The BER performance curves of the BMST-LDPC codes with different selection matrices are shown in Fig. 6, where we observe that the BMST-LDPC code using the 5G-NR LDPC-BC as the basic code with a selection matrix $\mathbf{S} = \mathbf{S}_d$ performs better than other selection matrices. The BER performance of the BMST-LDPC code ($\mathbf{S} = \mathbf{S}_d$) exhibits about 0.4 dB coding gain over the 5G-NR LDPC-BC at the BER of 10^{-5} . Therefore, for the BMST-LDPC code using the 5G-NR LDPC-BC as the basic code, selection matrix \mathbf{S}_d can be considered for partial superposition. In general, the BMST-LDPC codes outperform the 5G-NR LDPC-BC, thanking to the superposition style coupling that results in a longer code with greater error-correction capacity.

C. Trade-Offs Between Performance and Latency

The following two examples are provided to show the trade-off between the decoding performance and the latency.

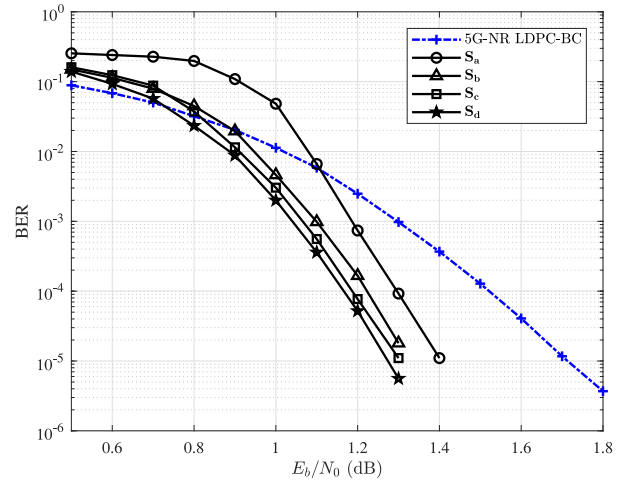


Fig. 6. BER performance of the BMST-LDPC codes with different \mathbf{S} . The superposition fraction for encoding is $\alpha = 384/1920$. The basic code is a rate-1/2 5G-NR LDPC-BC with a length of 1920 bits.

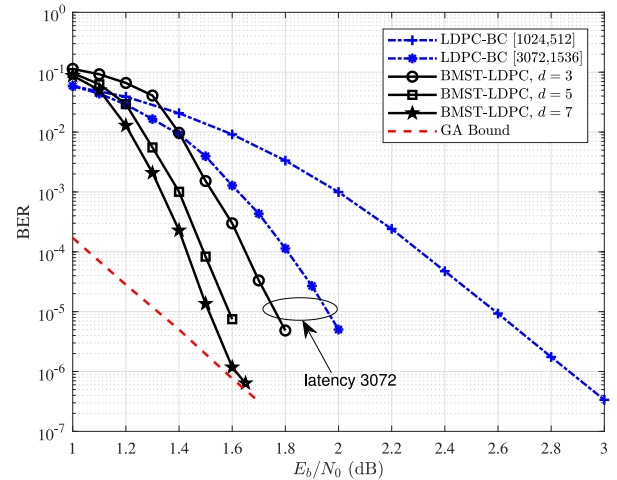


Fig. 7. BER performance of the BMST-LDPC codes with different d . The basic code is a rate-1/2 (3, 6)-regular LDPC-BC with a length of 1024 bits. The superposition fraction for encoding is $\alpha = 409/1024$, and the decoding window sizes are $d = 3, 5$ and 7 .

Example 3. (AWGN Channel, Varying d): Consider a rate-1/2 (3, 6)-regular LDPC-BC with a length of 1024 bits as the basic code. Codewords $c^{(t)}$ are transmitted with BPSK modulation over the AWGN channel. For comparison, we also simulate a rate-1/2 (3, 6)-regular LDPC-BC with a length of 1024 bits and a rate-1/2 (3, 6)-regular LDPC-BC with a length of 3072 bits. The BER performance comparison is shown in Fig. 7, where we observe that the performance of the BMST-LDPC code can be improved by increasing the window size d . However, the improvement saturates with an asymptotic performance approaching the GA bound [6], [12]. We also observe that the BMST-LDPC code can outperform the benchmark LDPC-BC with the same decoding latency, achieving an extra coding gain of about 0.5 dB at BER $\approx 10^{-5}$.

Example 4. (Fast Fading Channel, Varying d): Consider the rate-1/2 5G-NR LDPC-BC that was used in **Example 2** as the

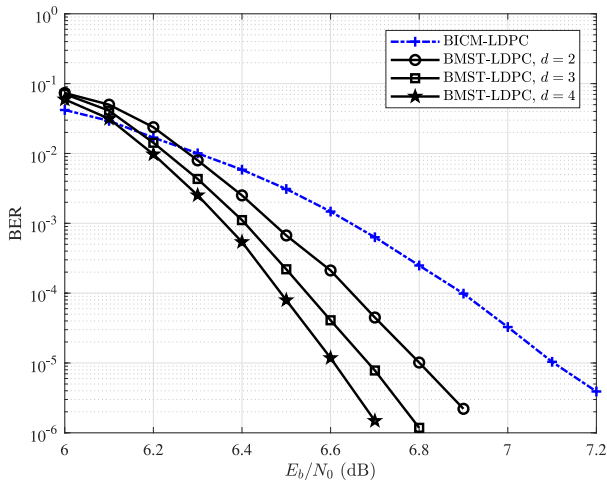


Fig. 8. BER performance of the BMST-LDPC code and BICM-LDPC code with 16-QAM constellation labeling Gray. The basic code is a rate-1/2 5G-NR LDPC-BC with a length of 1920 bits. The superposition fraction $\alpha = 384/1920$ and the selection matrix $\mathbf{S} = \mathbf{S}_d$.

basic code. Codewords $\mathbf{c}^{(t)}$ are transmitted using the 16-QAM with Gray labelling over the fast fading channel. For comparison, we also simulate the bit-interleaved coded modulation with LDPC (BICM-LDPC) code with the same 5G-NR LDPC-BC. The BER performance comparison is shown in Fig. 8, where we observe that the BMST-LDPC code achieves 0.3 dB, 0.4 dB, and 0.5 dB coding gains over the BICM-LDPC at the BER of 10^{-5} , by using windows of sizes 2, 3, and 4, respectively. As discussed in **Example 2**, the BMST-LDPC code outperforms the BICM-LDPC scheme due to the superposition style coupling which results in a better performance. We also observe that the performance of the BMST-LDPC code can be improved by increasing the window size d . Therefore, we can trade off the decoding performance against the latency.

D. Complexity Analysis

For the complexity insight of the proposed BMST-LDPC coding scheme, we use the complexity of the basic LDPC-BC as the comparison benchmark. For the encoding of the BMST-LDPC code, α extra binary additions per coded bit are needed. For the decoding, without considering earlier stopping, it is required to perform the decoding of the basic LDPC-BC $2 \sim d J_{\max} I_{\max}$ times. In our simulations, the parity-check based stopping criterion is used. We measure the complexity in terms of the average number of iterations for performing the decoding of the basic LDPC-BC.

Example 5. (Average Number of Iterations): We compare the average number of iterations for performing the decoding of the basic LDPC-BC between the BMST-LDPC code and the independent transmission of the LDPC-BC, as shown in Fig. 9. The basic code is the LDPC-BC used in **Example 3**. Codewords $\mathbf{c}^{(t)}$ are transmitted with BPSK modulation over the AWGN channel. The superposition fraction $\alpha = 409/1024$. Fig. 9 shows that the BMST-LDPC code exhibits a higher decoding iteration number when the SNR is low. However, this number will converge to that of the independent transmission of the LDPC-BC scheme as the

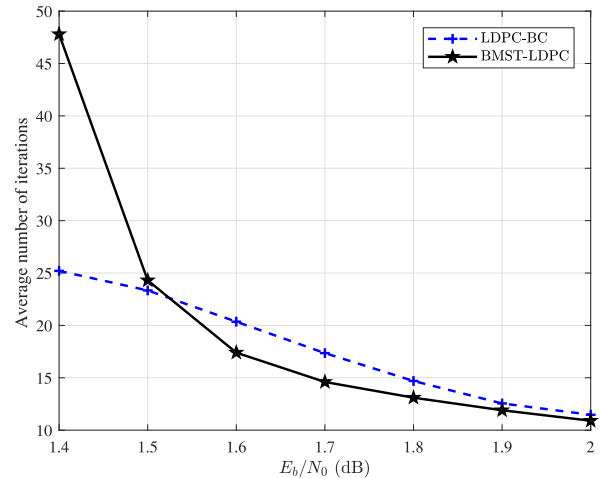


Fig. 9. The average number of iterations for performing the decoding of the basic LDPC-BC. The window size is $d = 3$. For the BMST-LDPC code, $J_{\max} = 50$ and $I_{\max} = 1$. For the independent transmission of the LDPC-BC, the maximum iteration number is 50.

SNR increases. That is, the complexity of the BMST-LDPC code is close to that of the LDPC-BC in the high SNR region. This is due to the better waterfall performance of the BMST-LDPC code and the parity-check based stopping criterion.

E. Applications to HARQ

The following two examples are provided to demonstrate the advantages of the BMST-LDPC HARQ scheme over the block fading channel. At the receiver, the parity check is used for error detection. For the BMST-LDPC HARQ, the maximum global iteration number is $J_{\max} = 2$ and the embedded basic LDPC-BCs are decoded by the SPA with a maximum iteration number of $I_{\max} = 25$. For the independent LDPC-BCs in the conventional RR-HARQ, the maximum iteration number is 50. Consider a rate-1/2 (3, 6)-regular LDPC-BC with a length of 1024 bits as the basic code. Codewords $\mathbf{c}^{(t)}$ are modulated using the BPSK modulation and transmitted over the block fading channel. The BMST-LDPC HARQ scheme that was summarized by Algorithm 4 is tested.

Example 6. (BMST-LDPC HARQ Scheme, Varying T_{\max}): In practical communication systems, since the end-to-end latency is always strictly constrained, the truncated HARQ protocols have been widely adopted, such as in 5 G system [50]. Taking the lossless BMST-LDPC HARQ scheme as a benchmark, we compare the truncated BMST-LDPC HARQ scheme with different maximum number of transmissions T_{\max} . For comparison, we have also simulated the conventional lossless RR-HARQ scheme using the same LDPC-BC. The throughput performance is shown in Fig. 10, from which we observe that the lossless BMST-LDPC HARQ scheme can yield a throughput improvement of up to 10% over the conventional lossless RR-HARQ scheme. We also observe that the throughput performance of the truncated BMST-LDPC HARQ scheme with $T_{\max} \geq 4$ is very closed to the lossless BMST-LDPC HARQ scheme. In order to achieve a good throughput performance and maintain

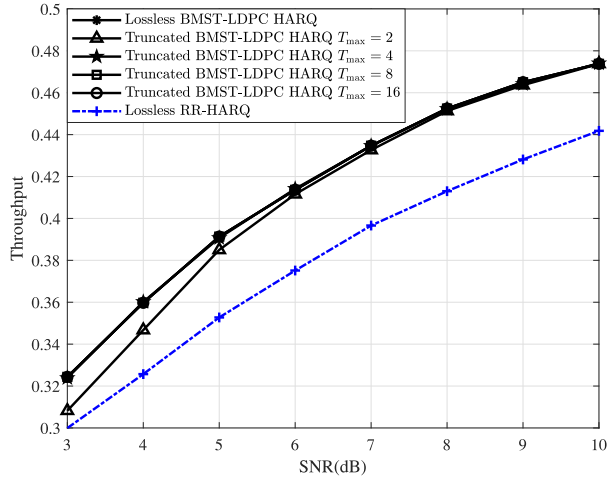


Fig. 10. Throughput performance of the BMST-LDPC HARQ scheme with different T_{max} . For the BMST-LDPC HARQ scheme, the superposition fraction $\alpha = 512/1024$. The basic code is a rate-1/2 (3, 6)-regular LDPC-BC with a length of 1024 bits.

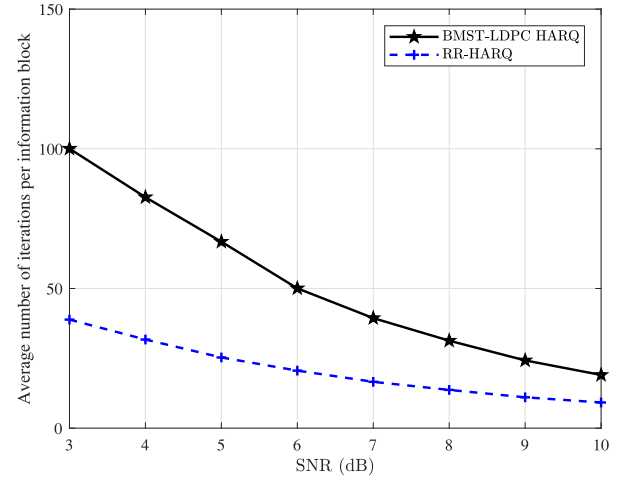


Fig. 12. The average number of iterations for performing the decoding of the LDPC-BC per information block. For the BMST-LDPC HARQ scheme and the conventional RR-HARQ, $T_{max} = 4$. In the BMST-LDPC HARQ scheme, $\alpha = 512/1024$, $J_{max} = 2$ and $I_{max} = 25$. In the RR-HARQ scheme, the maximum iteration number is 50.

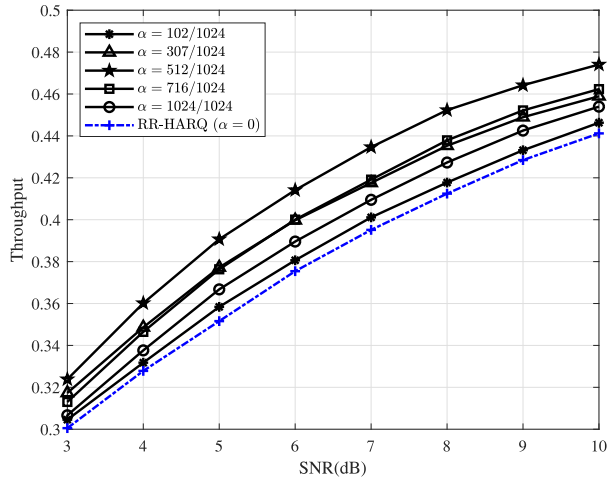


Fig. 11. Throughput performance of the BMST-LDPC HARQ scheme with different α . For the BMST-LDPC HARQ scheme and the conventional RR-HARQ scheme, $T_{max} = 4$. The basic code is a rate-1/2 (3, 6)-regular LDPC-BC with a length of 1024 bits.

a small latency, our results show that $T_{max} = 4$ yields the best compromise.

Example 7. (BMST-LDPC HARQ Scheme, Varying α): Using the one-dimensional search with a step size of 0.1 for the superposition fraction α , our simulation results for the BMST-LDPC HARQ scheme with $T_{max} = 4$ are shown in Fig. 11. For comparison, we have also simulated the conventional truncated RR-HARQ scheme using the same LDPC-BC with $T_{max} = 4$. Fig. 11 shows that in the truncated case, the proposed BMST-LDPC HARQ scheme with $\alpha = 512/1024$ can yield a throughput improvement of up to 10% over the conventional RR-HARQ scheme. It also confirms that the throughput performance can be improved from partial superposition with an optimized superposition fraction α .

We have also compared the complexity between the BMST-LDPC HARQ scheme and the conventional RR-HARQ scheme.

The complexity is measured in terms of the average number of iterations for performing the decoding of the LDPC-BC per information block, which in our simulations is obtained by counting the number of iterations over the subgraph corresponding to the LDPC-BC. When the decoding algorithm (Algorithm 2) of the BMST-LDPC codes is activated, each global iteration needs to be counted twice since two consecutive codewords of the LDPC-BC are involved. Notice that the parity-check stopping criterion is used in both the BMST-LDPC HARQ scheme and the conventional RR-HARQ scheme. Fig. 12 shows that in the high SNR region, the BMST-LDPC HARQ scheme incurs only a mild increase of the average iteration number. That is, the proposed BMST-LDPC HARQ scheme would not incur a large increase in complexity over the conventional RR-HARQ scheme in the high SNR region.

V. CONCLUSION

This paper has presented a new class of spatially coupled codes, which are constructed by sending codewords of an LDPC-BC in a BMST manner with partial superposition. The proposed BMST-LDPC codes can be implemented with the hardware basis of the corresponding LDPC-BCs. Moreover, the construction is universal in the sense that any existing LDPC-BCs can be used to construct the BMST-LDPC codes. We have presented a protograph-based EXIT chart analysis to predict the optimal superposition fraction of the BMST-LDPC codes. We have also proposed the BMST-LDPC HARQ scheme to improve the throughput performance over the block fading channel. Our numerical results have shown that the BMST-LDPC codes can obtain a coding gain of up to 1.0 dB over the underlying LDPC-BCs. They have also shown that the proposed BMST-LDPC HARQ scheme can have a throughput improvement of up to 10% over the original HARQ scheme.

REFERENCES

- [1] R. Gallager, "Low-density parity-check codes," *IRE Trans. Inf. Theory*, vol. 8, no. 1, pp. 21–28, Jan. 1962.
- [2] D. J. C. MacKay and R. M. Neal, "Near Shannon limit performance of low density parity check codes," *Electron. Lett.*, vol. 32, no. 18, pp. 1645–1646, Aug. 1996.
- [3] D. A. Spielman, "Linear-time encodable and decodable error-correcting codes," *IEEE Trans. Inf. Theory*, vol. 42, no. 6, pp. 1723–1731, Nov. 1996.
- [4] T. J. Richardson, M. A. Shokrollahi, and R. L. Urbanke, "Design of capacity-approaching irregular low-density parity-check codes," *IEEE Trans. Inf. Theory*, vol. 47, no. 2, pp. 619–637, Feb. 2001.
- [5] 3GPP, "Final report of 3GPP TSG RAN WG1 #87 v1.0.0, 3GPP," Tech. Rep., Feb. 2017. [Online]. Available: http://www.3gpp.org/ftp/tsg_ran/WG1_RL1/TSGR1_87/Report/
- [6] X. Ma, C. Liang, K. Huang, and Q. Zhuang, "Block Markov superposition transmission: Construction of big convolutional codes from short codes," *IEEE Trans. Inf. Theory*, vol. 61, no. 6, pp. 3150–3163, Jun. 2015.
- [7] C. Liang, X. Ma, Q. Zhuang, and B. Bai, "Spatial coupling of generator matrices: A general approach to design good codes at a target BER," *IEEE Trans. Commun.*, vol. 62, no. 12, pp. 4211–4219, Dec. 2014.
- [8] X. Ma, K. Huang, and B. Bai, "Systematic block Markov superposition transmission of repetition codes," *IEEE Trans. Inf. Theory*, vol. 64, no. 3, pp. 1604–1620, Mar. 2018.
- [9] S. Zhao and X. Ma, "Partially block Markov superposition transmission of a Gaussian source with nested lattice codes," *IEEE Trans. Commun.*, vol. 64, no. 12, pp. 5217–5226, Dec. 2016.
- [10] X. Mu, B. Bai, and R. Zhang, "Multiplicative repetition based superposition transmission of nonbinary codes," in *Proc. IEEE Int. Symp. Inf. Theory*, Barcelona, Spain, Jul. 2016, pp. 3023–3027.
- [11] X. Tan *et al.*, "Multiplicative repetition-based partial superposition transmission with nonbinary codes," in *Proc. IEEE Int. Symp. Turbo Codes Iterative Inform.*, Hong Kong, Dec. 2018, pp. 1–5.
- [12] Q. Wang *et al.*, "Spatially coupled LDPC codes via partial superposition," in *Proc. IEEE Int. Symp. Inf. Theory*, Paris, France, Jul. 2019, pp. 2614–2618.
- [13] A. J. Felstrom and K. S. Zigangirov, "Time-varying periodic convolutional codes with low-density parity-check matrix," *IEEE Trans. Inf. Theory*, vol. 45, no. 6, pp. 2181–2191, Sep. 1999.
- [14] S. Kudekar, T. Richardson, and R. Urbanke, "Spatially coupled ensembles universally achieve capacity under belief propagation," *IEEE Trans. Inf. Theory*, vol. 59, no. 12, pp. 7761–7813, Dec. 2013.
- [15] M. Lentmaier, A. Sridharan, D. J. Costello, and K. S. Zigangirov, "Iterative decoding threshold analysis for LDPC convolutional codes," *IEEE Trans. Inf. Theory*, vol. 56, no. 10, pp. 5274–5289, Oct. 2010.
- [16] S. Kudekar, T. Richardson, and R. Urbanke, "Threshold saturation via spatial coupling: Why convolutional LDPC ensembles perform so well over the BEC," *IEEE Trans. Inf. Theory*, vol. 57, no. 2, pp. 803–834, Feb. 2011.
- [17] A. R. Iyengar, M. Papaleo, P. H. Siegel, J. K. Wolf, A. Vanelli-Coralli, and G. E. Corazza, "Windowed decoding of protograph-based LDPC convolutional codes over erasure channels," *IEEE Trans. Inf. Theory*, vol. 58, no. 4, pp. 2303–2320, Apr. 2012.
- [18] A. E. Pusane, R. Smarandache, P. O. Vontobel, and D. J. Costello, "Deriving good LDPC convolutional codes from LDPC block codes," *IEEE Trans. Inf. Theory*, vol. 57, no. 2, pp. 835–857, Feb. 2011.
- [19] D. G. M. Mitchell, M. Lentmaier, and D. J. Costello, "Spatially coupled LDPC codes constructed from protographs," *IEEE Trans. Inf. Theory*, vol. 61, no. 9, pp. 4866–4889, Sep. 2015.
- [20] M. H. Tadayon, A. Tasdighi, M. Battagliioni, M. Baldi, and F. Chiaraluce, "Efficient search of compact QC-LDPC and SC-LDPC convolutional codes with large girth," *IEEE Commun. Lett.*, vol. 22, no. 6, pp. 1156–1159, Jun. 2018.
- [21] M. Battagliioni, A. Tasdighi, G. Cancellieri, F. Chiaraluce, and M. Baldi, "Design and analysis of time-invariant SC-LDPC convolutional codes with small constraint length," *IEEE Trans. Commun.*, vol. 66, no. 3, pp. 918–931, Mar. 2018.
- [22] M. Battagliioni, M. Baldi, F. Chiaraluce, and M. Lentmaier, "Girth properties of time-varying SC-LDPC convolutional codes," in *Proc. IEEE Int. Symp. Inf. Theory*, Paris, France, Jul. 2019, pp. 2599–2603.
- [23] S. Naseri and A. H. Banihashemi, "Spatially coupled LDPC codes with small constraint length and low error floor," *IEEE Commun. Lett.*, vol. 24, no. 2, pp. 254–258, Feb. 2020.
- [24] S. Mo, L. Chen, D. J. Costello, D. G. M. Mitchell, R. Smarandache, and J. Qiu, "Designing protograph-based quasi-cyclic spatially coupled LDPC codes with large girth," *IEEE Trans. Commun.*, vol. 68, no. 9, pp. 5326–5337, Sep. 2020.
- [25] K. Liu, M. El-Khamy, and J. Lee, "Finite-length algebraic spatially-coupled quasi-cyclic LDPC codes," *IEEE J. Sel. Areas Commun.*, vol. 34, no. 2, pp. 329–344, Feb. 2016.
- [26] M. Sadeghi, "Optimal search for girth-8 quasi cyclic and spatially coupled multiple-edge LDPC codes," *IEEE Commun. Lett.*, vol. 23, no. 9, pp. 1466–1469, Sep. 2019.
- [27] K. Huang and X. Ma, "Performance analysis of block markov superposition transmission of short codes," *IEEE J. Sel. Areas Commun.*, vol. 34, no. 2, pp. 362–374, Feb. 2016.
- [28] A. E. Pusane, A. J. Felstrom, A. Sridharan, M. Lentmaier, K. S. Zigangirov, and D. J. Costello, "Implementation aspects of LDPC convolutional codes," *IEEE Trans. Commun.*, vol. 56, no. 7, pp. 1060–1069, Jul. 2008.
- [29] G. D. Forney, "Codes on graphs: Normal realizations," *IEEE Trans. Inf. Theory*, vol. 47, no. 2, pp. 520–548, Feb. 2001.
- [30] G. Liva and M. Chiani, "Protograph LDPC codes design based on EXIT analysis," in *Proc. IEEE Glob. Commun. Conf.*, Washington, DC, USA, Nov. 2007, pp. 3250–3254.
- [31] M. Battagliioni, M. Baldi, and E. Paolini, "Complexity-constrained spatially coupled LDPC codes based on protographs," in *Proc. Int. Symp. Wireless Commun. Syst.*, Bologna, Italy, Aug. 2017, pp. 49–53.
- [32] S. ten Brink, "Convergence behavior of iteratively decoded parallel concatenated codes," *IEEE Trans. Commun.*, vol. 49, no. 10, pp. 1727–1737, Oct. 2001.
- [33] S. Ten Brink, G. Kramer, and A. Ashikhmin, "Design of low-density parity-check codes for modulation and detection," *IEEE Trans. Commun.*, vol. 52, no. 4, pp. 670–678, Apr. 2004.
- [34] X.-Y. Hu, E. Eleftheriou, and D. M. Arnold, "Regular and irregular progressive edge-growth Tanner graphs," *IEEE Trans. Inf. Theory*, vol. 51, no. 1, pp. 386–398, Jan. 2005.
- [35] I. Sutskever, S. Shamaï, and J. Ziv, "Extremes of information combining," *IEEE Trans. Inf. Theory*, vol. 51, no. 4, pp. 1313–1325, Apr. 2005.
- [36] G. Benelli, "An ARQ scheme with memory and soft error detectors," *IEEE Trans. Commun.*, vol. 33, no. 3, pp. 285–288, Mar. 1985.
- [37] D. Chase, "Code combining - A maximum-likelihood decoding approach for combining an arbitrary number of noisy packets," *IEEE Trans. Commun.*, vol. 33, no. 5, pp. 385–393, May 1985.
- [38] J. Hagenauer, "Rate-compatible punctured convolutional codes (RCPC codes) and their applications," *IEEE Trans. Commun.*, vol. 36, no. 4, pp. 389–400, Apr. 1988.
- [39] D. M. Mandelbaum, "An adaptive-feedback coding scheme using incremental redundancy," *IEEE Trans. Inf. Theory*, vol. 20, no. 3, pp. 388–389, May 1974.
- [40] C. Hausl and A. Chindapol, "Hybrid ARQ with cross-packet channel coding," *IEEE Commun. Lett.*, vol. 11, no. 5, pp. 434–436, May 2007.
- [41] J. Chui and A. Chindapol, "Design of cross-packet channel coding with low-density parity-check codes," in *Proc. IEEE Inf. Theory Workshop Inf. Theory Wireless Netw.*, Jul. 2007, pp. 1–5.
- [42] M. Jabi, A. Benyouss, M. Le Treust, É. Pierres-Doray, and L. Szczecinski, "Adaptive cross-packet HARQ," *IEEE Trans. Commun.*, vol. 65, no. 5, pp. 2022–2035, May 2017.
- [43] G. Cocco and D. Floreano, "Cross-packet coding for delay-constrained streaming applications," *IEEE Commun. Lett.*, vol. 23, no. 11, pp. 1962–1966, Nov. 2019.
- [44] R. Zhang and L. Hanzo, "Superposition-coding-aided multiplexed hybrid ARQ scheme for improved end-to-end transmission efficiency," *IEEE Trans. Veh. Technol.*, vol. 58, no. 8, pp. 4681–4686, Oct. 2009.
- [45] R. Zhang and L. Hanzo, "Superposition-aided delay-constrained hybrid automatic repeat request," *IEEE Trans. Veh. Technol.*, vol. 59, no. 4, pp. 2109–2115, May 2010.
- [46] Y. Lang, D. Wübben, A. Dekorsy, V. Braun, and U. Doetsch, "Improved HARQ based on network coding and its application in LTE," in *Proc. IEEE Wireless Commun. Netw. Conf.*, Shanghai, China, Apr. 2012, pp. 1958–1963.
- [47] J. Manssour, A. Osseiran, and S. B. Slimane, "A unicast retransmission scheme based on network coding," *IEEE Trans. Veh. Technol.*, vol. 61, no. 2, pp. 871–876, Feb. 2012.
- [48] G. Caire and D. Tuninetti, "The throughput of hybrid-ARQ protocols for the Gaussian collision channel," *IEEE Trans. Inf. Theory*, vol. 47, no. 5, pp. 1971–1988, Jul. 2001.

- [49] D. G. M. Mitchell, M. Lentmaier, A. E. Pusane, and D. J. Costello, "Randomly punctured LDPC codes," *IEEE J. Sel. Areas Commun.*, vol. 34, no. 2, pp. 408–421, Feb. 2016.
- [50] 3GPP, "Multiplexing and channel coding (Release 15)," 3GPP TS 38.212 V15.1.1, Apr. 2018. [Online]. Available: https://www.3gpp.org/ftp/Specs/archive/38_series/38.212/38212-f11.zip



Qianfan Wang (Student Member, IEEE) received the B.S. degree in applied physics from Henan Polytechnic University, Jiaozuo, China, in 2014 and the M.S. degree in 2017 in electronics and communication engineering from Sun Yat-sen University, Guangzhou, China, where he is currently working toward the Ph.D. degree. His research interests include information theory, channel coding theory, and their applications to communication systems.



Suihua Cai received the B.Sc. degree in information and computer science from the China University of Geosciences, Wuhan, China, in 2011, and the M.S. degree in fundamental mathematics and the Ph.D. degree in information and communication engineering from Sun Yat-sen University, Guangzhou, China, in 2016 and 2019, respectively. He is currently a Postdoctoral Fellow with Sun Yat-sen University. His research interests include information theory, channel coding theory, and their applications to communication systems.



Wenchao Lin received the B.E. degree in communication engineering and the M.Sc. degree in computer science and technology from Sun Yat-sen University, Guangzhou, China, in 2017 and 2020, respectively. His current research interests include channel coding theory and its application to communication systems.



Shancheng Zhao received the bachelor's degree in software engineering and Ph.D. degree in communication and information systems from Sun Yat-sen University, Guangzhou, China, in 2009 and 2014, respectively. He is currently a Professor with the College of Information Science and Technology, Jinan University, Guangzhou, China. From 2013 to 2014, he was a Graduate Visiting Student with the University of California, Los Angeles, Los Angeles, CA, USA. His current research interests include spatially coupled codes and their applications. He was the

co-recipient of the Best Paper Award of 2015 IEEE GlobeCom. He is also an Associate Editor for *IET Quantum Communication* and *Elsevier Physical Communication*.



Li Chen (Senior Member, IEEE) received the B.Sc. degree in applied physics from Jinan University, Guangzhou, China, in 2003, and the M.Sc. degree in communications and signal processing and the Ph.D. degree in communications engineering from Newcastle University, Newcastle upon Tyne, U.K., in 2004 and 2008, respectively. From 2007 to 2010, he was a Research Associate with Newcastle University. In 2010, he returned to China as a Lecturer with the School of Information Science and Technology, Sun Yat-sen University, Guangzhou, China. From 2011 to 2012, he was a Visiting Researcher with the Institute of Network Coding, The Chinese University of Hong Kong, Hong Kong. From 2011 and 2016, he was an Associate Professor and a Professor with University. Since 2013, he has been the Associate Head of the Department of Electronic and Communication Engineering. From July 2015 to October 2015, he was a Visitor with the Institute of Communications Engineering, Ulm University, Ulm, Germany. From October 2015 to June 2016, he was a Visiting Associate Professor with the Department of Electrical Engineering, University of Notre Dame, Notre Dame, IN, USA. From 2017 to 2020, he was the Deputy Dean of the School of Electronics and Communication Engineering. His research interests include information theory, error-correction codes, and data communications. He likes reading and photography. He is a Senior Member of the Chinese Institute of Electronics (CIE). He is a Member of the IEEE Information Theory Society Board of Governors Conference Committee, the Chair of the IEEE Information Theory Society Guangzhou Chapter, and a Committee Member of the CIE Information Theory Society. He is currently an Associate Editor for IEEE TRANSACTIONS ON COMMUNICATIONS. He has been involved in organizing several international conferences, including the 2018 IEEE Information Theory Workshop at Guangzhou, for which he was the General Co-Chair.



Xiao Ma (Member, IEEE) received the Ph.D. degree in communication and information systems from Xi-dian University, Xi'an, China, in 2000. He is currently a Professor with the School of Computer Science and Engineering, Sun Yat-sen University, Guangzhou, China. From 2000 to 2002, he was a Postdoctoral Fellow with Harvard University, Cambridge, MA, USA. From 2002 to 2004, he was a Research Fellow with the City University of Hong Kong, Hong Kong. His research interests include information theory, channel coding theory, and their applications to communication systems and digital recording systems. He was the co-recipient, with A. Kavčić and N. Varnica, of the 2005 IEEE Best Paper Award in Signal Processing and Coding for Data Storage.